

## Particle emission measurements in three scenarios of mechanical degradation of polypropylene-nanoclay nanocomposites

María Blazquez<sup>a,b</sup>, Verónica Marchante<sup>c</sup>, Laura Gendre<sup>c,1</sup>, Kristof Starost<sup>d</sup>, James Njuguna<sup>d</sup>, Jurg A. Schutz<sup>e</sup>, José María Lacave<sup>b</sup>, Ainhoa Egizabal<sup>f</sup>, Cristina Elizetxea<sup>f</sup>, Miren P. Cajaraville<sup>b,\*</sup>

<sup>a</sup> INKOA SISTEMAS, SL, Ribera de Axpe 11, Edificio D1, Dpto 208, 48950, Erandio, Bizkaia, Spain

<sup>b</sup> CBET Research Group, Department of Zoology and Animal Cell Biology, Faculty of Science and Technology and Research Centre for Experimental Marine Biology and Biotechnology PiE, University of the Basque Country UPV/EHU, Barrio Sarriena S/n., 48940, Leioa, Bizkaia, Spain

<sup>c</sup> Advanced Vehicle Engineering Centre, School of Aerospace, Transport and Manufacturing, Cranfield University, MK43 0AL, Bedfordshire, UK

<sup>d</sup> Centre for Advanced Engineering Materials, School of Engineering, Robert Gordon University, AB10 7GJ, Aberdeen, UK

<sup>e</sup> Commonwealth Scientific and Industrial Research Organisation (CSIRO), Deakin Mail Centre Building LA, 75 Pigdons Road, Waurn Ponds, VIC 3216, Australia

<sup>f</sup> TECNALIA, Mikeletegi Pasealekua, 2, E-20009, Donostia, Spain

### ARTICLE INFO

#### Keywords:

Polymer nanocomposite  
Nanoclays  
Mechanical degradation  
Particle emission  
Exposure assessment

### ABSTRACT

Researchers and legislators have both claimed the necessity to standardize the exposure assessment of polymer nanocomposites throughout their life cycle. In the present study we have developed and compared three different and independent operational protocols to investigate changes in particle emission behavior of mechanically degraded polypropylene (PP) samples containing different fillers, including talc and two types of nanoclays (wollastonite-WO- and montmorillonite-MMT-) relative to not reinforced PP. Our results have shown that the mechanical degradation of PP, PP-Talc, PP-WO and PP-MMT samples causes the release of nano-sized particles. However, the three protocols investigated, simulating industrial milling and drilling and household drilling, have produced different figures for particles generated. Results suggest that it is not possible to describe the effects of adding nano-sized modifiers to PP by a single trend that applies consistently across all different protocols. Differences observed might be attributed to a variety of causes, including the specific operational parameters selected for sample degradation and the instrumentation used for airborne particle release characterization. In particular, a streamlined approach for future assessments providing a measure for released particles as a function of the quantity of removed material would seem useful, which can provide a reference benchmark for the variations in the number of particles emitted across a wider range of different mechanical processes.

### 1. Introduction

In material science, the incorporation of nanoclays, comprising e.g. layered mineral silicates, into thermoplastics can lead to

\* Corresponding author.

E-mail address: [mirenp.cajaraville@ehu.eus](mailto:mirenp.cajaraville@ehu.eus) (M.P. Cajaraville).

<sup>1</sup> Present address: WMG, University of Warwick, University Road, CV4 7AL, Coventry (West Midlands) United Kingdom.

<https://doi.org/10.1016/j.jaerosci.2020.105629>

Received 3 April 2020; Received in revised form 29 July 2020; Accepted 31 July 2020

Available online 14 August 2020

0021-8502/© 2020 The Authors. Published by Elsevier Ltd. This is an open access article under the CC BY-NC-ND license

(<http://creativecommons.org/licenses/by-nc-nd/4.0/>).

improved barrier properties, flame retardance, and mechanical properties, depending on the choice of filler. Wollastonite (WO) and montmorillonite (MTT) represent two types of widely used nanofillers to develop lighter weight structural parts for the automotive industry. WO is an effective and low-cost filler that can improve the tensile modulus, stiffness, hardness and strength of polymers (Ding et al., 2012). Other key characteristics of WO include good thermal stability, low water absorption and relatively low health hazard risk (Balkan et al., 2010). Exfoliated MMT is most popular for use in polymers because of its high surface area and surface reactivity, which both together lead to improved mechanical properties (tensile, hardness, impact, strength, etc.). Although the toxicological potential of this type of materials is generally considered low, Verma et al. (2012) have found in their evaluation of the cytotoxicity of nanoclays with different morphologies (platelet and tubular) on human lung epithelial cells A549 the occurrence of varying degrees of dose- and time-dependent cytotoxic effects, which apply to both nanoclay types. Janer et al. (2013) compared the *in vitro* effects of commercially available nanoclays for a series of cell lines, including A549, and concluded that toxicological effects were in fact related to the presence of organic modifiers used to exfoliate the platelets. Exposure to nanoclays may therefore cause toxicological effects in pulmonary cell lines, which vary depending on the type of nanoclay used, the presence of organic modifiers and their dosage. As a consequence, it is of utmost importance to evaluate the health risk potential of layered silicates, embedded either in a polymer composite matrix or bound to the material surface, when released into the air during normal wear and tear or as a result of an emergency.

Several studies have adopted a life-cycle oriented approach to address the safety concerns that are attributed to solid nanocomposites. A variety of reviews evaluate the literature investigating the release of ENMs from polymer nanocomposites during product manufacture, consumer use and end of life (EOL) scenarios. Froggett et al. (2014) identified fifty-four studies, which evaluated the release of nanomaterials from solid, non-food nanocomposites, and grouped them according to specific scenarios: machining, weathering, washing, contact and incineration. Authors concluded that release from nanocomposites can take on various forms and highlighted the need to standardize experiments for comparative release assessment. Schlagenhauf et al. (2014) summarized investigations concerned with the release of carbon nanotubes (CNTs) from nanocomposites during the service life and concluded that studies investigating the release caused by mechanical impact factors do not provide a consistent picture. Duncan (2015), having evaluated the existing knowledge in relation to the potential release of ENMs from polymer nanocomposites, pointed out a primary limitation of the studies conducted so far as having poorly characterized materials employed in the investigations, hence hindering the reliable formulation of predictive frameworks for ENM release phenomena. More recently, Ding et al. (2017a) claimed as a limitation in the existing literature the absence of information concerning the properties and amounts of raw materials handled and the need to collect data in an harmonized approach so as to calculate the real release rates of the process concerned.

In the present study we have selected samples from nanocomposite materials that comprise a polypropylene (PP) matrix, which is one of the most widely used composition for commodity thermoplastics in automotive applications. This is because the low density of PP provides weight saving, helps to improve fuel economy and reduces cost (Jansz, 1999). WO and MMT have been reported to be dispersed in PP for the purpose of decreasing density while maintaining favourable mechanical properties (Gonzalez et al., 2014; Salas-Papayanopolos et al., 2014).

The first objective of this investigation was to develop three different scenarios that simulate the use and EOL phase of PP samples containing different fillers, including talc and two types of nanoclays (WO, MMT). The scenarios include industrial milling and drilling as well as household drilling at spindle speeds of 1250, 8500 and 10000 rpm and feed rates of 16, 200 and 78 mm/min, respectively. All scenarios have been carried out in confined conditions to suppress ambient particle background. A second objective was concerned with comparing particle emission profiles for the nanofilled samples in contrast to the reference samples (neat PP and talc containing PP) within a particular scenario, followed by comparing results among the three scenarios.

The development of scenarios simulating emissions at different life cycle stages is generally regarded as the first step in a broader nano-release investigation, leading the way towards a standardized approach of exposure assessment throughout the life cycle of nanocomposites.

## 2. Materials and methods

### 2.1. Materials and samples preparation

Reference materials included a commercially available polypropylene (PP) homopolymer (Moplen HP648T) and a 20% talc filled PP copolymer (Holstacom XM 2416) both purchased from Lyondell Basell Industries (Houston, USA). The reinforcements and concentrations chosen were 5% wt. WO (Harwoll 7ST5) from Nordkalk (Pargas, Finland) and 5% wt. MMT (Nanomer I30T) from Nanocor Corporation (Illinois, USA). The ZSK 26 MEGA compounder twin-screw extruder from Coperion (Stuttgart, Germany) was used for homogenization of the nanocomposite samples. For samples containing WO and MMT, extrusion parameters were 800 rpm screw speed and lateral feeding type. The extruded pellets of the materials were injection moulded by means of an All Rounder 270C-300-100 Injection Moulding Machine from Arburg (Loßburg, Germany). Due to large differences in chemical polarity between PP and MMT or WO, maleic anhydride was mixed into the PP as a coupling agent (MAPP, Polybond 3200 from Addviant, Connecticut, USA). Using MAPP would ensure good interfacial adhesion between the nanofillers and the polymer. Therefore, four sets of samples were fabricated: neat PP, PP with 20% wt. talc (PP-Talc), PP with 5% wt. MMT and 2% wt. coupling agent (PP-MMT), and PP with 5% wt. WO with 2% wt. coupling agent (PP-WO). Pellets from the four samples were injection moulded into standard test specimens for tensile mechanical evaluation according to ISO 527 (International Organization for Standardization, 2019).

Measurements of modulus, strength and density resulted in  $2417.6 \pm 27$  MPa,  $25.12 \pm 0.4$  MPa and  $1.035$  g/cm<sup>3</sup> for PP-Talc,  $2408.8 \pm 6.9$  MPa,  $24.8 \pm 0.4$  MPa and  $0.935$  g/cm<sup>3</sup> for PP-WO and  $1074.2 \pm 16.1$  MPa,  $23.36 \pm 0.3$  MPa and  $0.942$  g/cm<sup>3</sup> for

PP-MMT. The characterization of mechanical sample properties revealed that the best performance was obtained by PP-WO, since the addition of only 5 wt% WO in PP achieved the same tensile strength to those of a 20 wt% talc in PP, resulting furthermore in a 10% lower material density saving. This implies that an automotive component can be manufactured with 10% less weight at equivalent mechanical performance. The neat PP sample was used as an additional reference to the PP-Talc sample.

2.2. Experimental set up representing a milling scenario in an industrial environment

The experimental set up corresponding to the industrial milling scenario was partially described in a publication by Schutz and

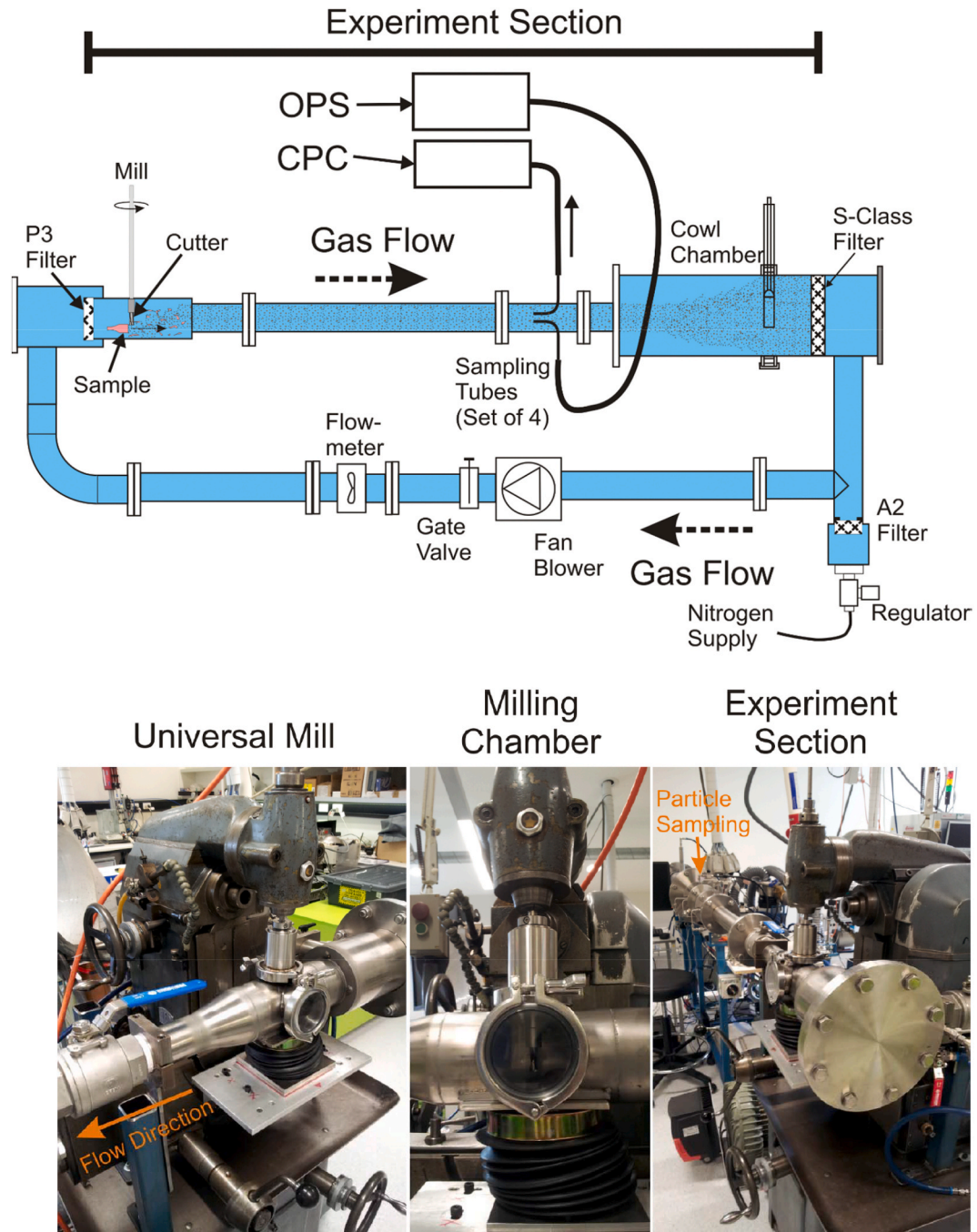


Fig. 1. A: Schematic diagram of the Test Duct. B: Images of the set-up used to simulate an industrial milling process and characterize the associated particle release.

Halliburton (2010). However, while the reported set up was employing an atomizer for the generation of particles, the dust particles from samples investigated in the present study were generated by mechanical degradation using a mill.

- (i) Environmental control: A hermetically sealed, torus-shaped circulating Test Duct configuration was used that contained nitrogen as medium for the aerosol. The test duct is a closed circuit where the gas flow inside is driven by a side-channel fan blower (Elektror). Particles released from the PP samples were picked up by the particle-free gas flowing through the duct. All composite samples were tested at a constant flow rate of 32 L/min. The Experiment Section was enclosed on both ends between high efficiency air filters: P3 Sundstroem SR510 upstream and vacuum cleaner S-Class filter (Electrolux) downstream, which remove >99.97% of particles from the airstream before the carrier gas was injected back into the milling chamber.
- (ii) Industrial automatic machining system: An Aciera F3 Universal Mill (Anglo-Swiss Tools, UK) with 10 mm diameter High-Speed Steel (HSS) mill-cutter was used to machine a 5 cm long section of the samples. Milling speed of 1250 rpm and feed rate of 16 mm/min were used. The cutting depth was by default 0.5 mm/pass, but the effect of slight deviations from this setting (0.25 or 0.76 mm/pass) was investigated in some milling events for the PP-Talc, PP-WO and PP-MMT samples. These events are marked respectively by labels 0.01" and 0.03" on the upper part of each graph in the results section.
- (iii) Particle release measurement: Airborne particles were picked up by sampling tubes and detected by two types of particle counters: a) Optical Particle Sizer (OPS) Model 3330 (TSI Inc., Minnesota, USA) – 16 channels from 300 to 10000 nm particle size and b) a Condensation Particle Counter (CPC) Model 3007 (TSI Inc., Minnesota, USA) – 1 channel from 10 to 1000 nm particle size. The OPS channel configuration "TSI Default" was used (Table S1).
- (iv) Data processing: While the OPS 3330 covers all particle size ranges from 300 to 10000 nm, the CPC 3007 covers particle size ranges from 10 to 1000 nm. Therefore an overlap takes place in the measurement ranges of these instruments between 300 and 1000 nm particle size and measurements of both instruments need to be combined in order to manage this overlap.

The OPS channel configuration "TSI Default" (S1) was used, which covers the whole measurement range in 16 channels of equal log-normal width, i.e.:

$$\text{OPS } \text{Log}_{10} \left( \frac{D_n^u}{D_n^l} \right) = \text{Log}_{10} \left( \frac{D_n^u}{d_u} \right) - \text{Log}_{10} \left( \frac{D_n^l}{d_u} \right) = 0.096 \quad (1)$$

for all  $n$  channels covering specific particles in a range upper and lower size limits given by the interval  $[D_n^u, D_n^l]$  and using unit constant  $d_u = 1 \mu\text{m}$ .

In order to adjust the scale of the data from the CPC in the range of 10–300 nm and make that data comparable to the OPS data, eq (1) has been used with different values that correspond to properties of the CPC:  $D_n^u = 0.3 \mu\text{m}$ ,  $D_n^l = 0.01 \mu\text{m}$  and using unit constant  $d_u = 1 \mu\text{m}$ , which provides a value of 1.477.

$$\text{CPC } \text{Log}_{10} \left( \frac{D_n^u}{D_n^l} \right) = \text{Log}_{10} \left( \frac{D_n^u}{d_u} \right) - \text{Log}_{10} \left( \frac{D_n^l}{d_u} \right) = 1.477 \quad (2)$$

Subsequently, the total CPC measured PNC (10–1000 nm) was scaled by  $\frac{1}{\text{Log}_{10}(D_p)}$ , multiplying data by  $0.096/1.477 = 0.065$ .

The next step involved adding up PNC values measured by OPS in a range of 300–1000 nm (number count of channels 1–5 and half the number count of channel 6, see Table S1).

Finally, the PNC measured by the CPC for 10–300 nm was calculated by subtracting the PNC measured by the OPS for 300–1000 nm from the PNC measured by the CPC for 10–1000 nm.

This size-normalization is represented in pertinent data plots as 'dN/dlogDp', which includes the PNC for 10–300 nm (CPC scaled data), 300–1000 nm (CPC and OPS combined figure) and 1000–10000 nm (OPS data).

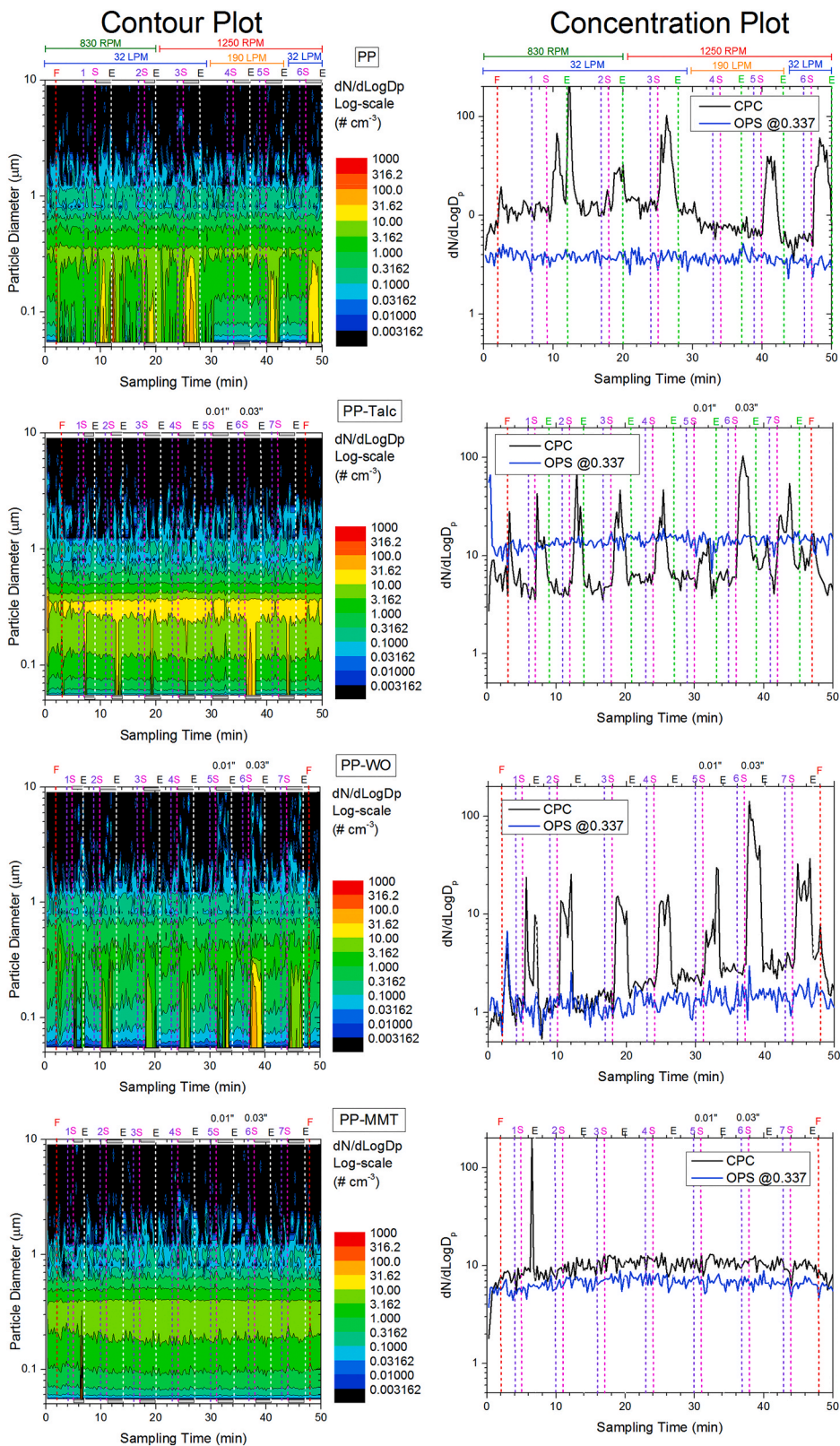
A simplified representation of the Test Duct is provided in Fig. 1 (A); the photos in Fig. 1 (B) illustrate implementation details. The operational protocol used to mill the nanocomposite samples comprised a series of successive steps, starting from turning on the gas flow and followed by a series of successive milling steps –generally 6–7 passes - taking the specimen in a continuous movement perpendicular to the mill cutter from the Start (S) to the End (E) points at an advance of 16 mm/min.

This represents, to the best of our knowledge, one of the first studies on the emissions associated to polymer nanocomposites milling.

### 2.3. Experimental set up representing a drilling scenario in an industrial environment

The experimental set up for industrial drilling was detailed by Gendre et al. (2016). Briefly, the main properties of the experimental set up were as follows:

- (i) Environmental control: A sealed chamber with a fan, model I100-4 (from BenchVent, Harrogate, UK) was used. The fan recirculated the air inside the chamber and a combination of pre-filter and HEPA filter (category H14) was used to remove particles from the air. An air recirculation system was operating in parallel to control chamber pressure. The spindle drill used for mechanical degrading was water cooled and totally enclosed in order to prevent the generation of background particles by the motor.



(caption on next page)

**Fig. 2.** From top to bottom: PSD (left) and PNC (right) expressed as  $dN/d\log D_p$  ( $\#/cm^3$ ) corresponding to airborne particle release measured using the protocol for simulated industrial milling processes produced by PP, PP-Talc, PP-WO and PP-MMT samples. Results in the contour plots on the left show measured number count concentrations graded according to a colour scale (see legend) as a function of time (abscissa) and particle diameter (ordinate). Temporal cross-sections from these contour plots are shown on the right, where concentration changes over time are shown for given particle sizes: black curves labelled “CPC” hereby refer to particles in a size range from 10 nm to 300 nm and blue curves labelled “OPS @0.337” refer to particles from 300 nm to 374 nm size, according to the respective OPS size-bin. Sections of milling actions are represented as grey bars at the bottom, corresponding to start (S) and end (E) markings at the top of the graph; periods where the mill cutter was not in contact with the sample are the white sections between grey bars. (For interpretation of the references to colour in this figure legend, the reader is referred to the Web version of this article.)

- (ii) Industrial automatic machining system: A Computer Numerical Control (CNC) machine was designed and built, which allowed precise control of drilling parameters via feed rate, spindle speed, etc. A High-Speed Steel (HSS) plain shank short drill bit of 3.5 mm diameter was used with a spindle speed of 8500 rpm and a feed rate of 200 mm/min.
- (iii) Particle release measurement: A scanning mobility particle sizer (‘SMPS + C’) from Grimm Aerosol (Ainring, Germany) was used to characterize the concentration and particle size distribution (PSD) of airborne nanoparticles released. The ‘SMPS + C’ comprises of a CPC model 5403 with a Vienna-type classifier, the long U-DMA. This equipment was connected to the chamber using antistatic hoses. The PSD measured ranges from 11.1 nm to 1083.8 nm and distributed across 44 channels.

In relation to the operational protocol, one requirement for the assessment of nanoparticles release was that the total drilling time had to be equal to the time that the SMPS + C needed to complete one full scan, i.e. 7 min. Reported data comprises pre-drilling (background), drilling and two successive measurements undertaken after drilling (stabilization). The airborne particle release measurements were replicated a minimum of three times for each sample.

Samples were weighted before and after particle release measurement in order to calculate the amount of material removed by the drilling.

#### 2.4. Experimental set up representing a drilling scenario in a household environment

The experimental set-up used for household drilling was described by Starost et al. (2017a, 2017b). Its main properties include:

- (i) Environmental control: A closed stainless steel chamber with dimensions of 740 mm × 550 mm × 90 mm was used as containment for the experiment. The chamber was initially cleared of particles before each test through an inflow of clean air with the use of Capsule HEPA Filters from TSI providing >99.97% particle retention.
- (ii) Automatic machining system: A drilling tool model 4000 from Dremel (Wisconsin, USA) with a standard stainless steel, 3.5 mm diameter twist drill bit was used at 10000 rpm with a feed rate of 78 mm/min. The tool was manually operated inside the chamber.
- (iii) Particle release measurement: The particle number concentration (PNC) was gathered using an Environmental Particle Counter (EPC, a water-based CPC) Model 3783 (TSI Inc., Minnesota, USA) at a flow rate of 0.6 L/min, across a particle range of 1–1000 nm and a concentration range of 0 to  $10^6$  particles/cm<sup>3</sup> with a reading accuracy of 0.01 particles/cm<sup>3</sup>. Using the EPC, the PNC was quantified in situ with a sampling rate of 1 Hz. An SMPS model 3080 (TSI Inc. Minnesota, USA) was used for PSD measurement. The instrument includes an electrostatic classifier utilizing a nano Differential Mobility Analyzer (DMA) with 99 distinct particle diameter channels within a particle range of 4.61–156.8 nm and a flow rate of 0.31 L/min.

Within the present scenario, particle measurements conducted before drilling was performed revealed the absence of background particles within the detection limits of the EPC. Subsequently, eight holes were drilled within 3 min, followed by 1 min of no drilling to allow particle concentrations to stabilize.

#### 2.5. Statistical analysis

Statistical analyses for the comparison of PNC values of samples tested within each of the operational protocols were performed using the SPSS statistical package v22.0 (SPSS Inc., Microsoft Co, WA, USA). Data were tested for normality (Kolmogorov-Smirnov test) and homogeneity of variances (Levene’s test). Then, the non-parametric Kruskal-Wallis test was applied, followed by the Dunn’s post hoc test. In all cases, significance was established at  $p < 0.05$ .

### 3. Results

#### 3.1. Results of the experimental set up representing a milling scenario in an industrial environment

As an initial step the sensitivity of the experimental set up was characterized. For this purpose, a measurement of the laboratory air was compared in Fig. S1 to the release generated by the milling actions on pure PP sample, showing that emissions from milling are below the natural ambient particle concentration levels.

Corresponding PSD contour plots and PNC time-scans from measurements conducted under exclusion of ambient background

particles are presented in Fig. 2. Results illustrate that particle emissions for all samples increased for particles <300 nm size during milling actions (sections between labels “S” and “E”, corresponding to those specific moments when the samples were being mechanically degraded). Fig. S2 shows details of the mechanically degraded samples.

Since particle distribution results from combined CPC and OPS data show that the only significant increases originate from <300 nm particle size fractions, which corresponds to the range from 10 to 300 nm that is covered by the CPC, the particle concentration in Table 1 has been calculated using CPC data only at 1250 rpm.

The nanoparticle-filled composite samples PP-WO and PP-MMT showed a 44.63% decrease and 73.24% decrease, respectively, for the average PNC emissions during milling events when compared to the emissions from the PP sample. The PP-Talc showed a decrease of 47.99% for the same comparison. Differences were significant ( $p < 0.05$ ) in all cases. Significant differences were also observed for the emissions corresponding to all PP-Talc, PP-WO and PP-MMT samples compared with PP sample when no milling was being conducted (stabilization) ( $p < 0.05$ ). Results therefore suggest that the presence of micro and nanofillers in the PP matrix was decreasing the concentration of emitted particles during mechanical degradation and during subsequent stabilization periods under the conditions tested.

When the comparison was carried out for the emissions of the two nanofilled composite samples relative to those of PP-Talc, the result was a 6.46% increase for PP-WO and a 48.54% decrease for PP-MMT, respectively, during milling actions, differences not being statistically significant. The differences observed during stabilization, however, were significant ( $p < 0.05$ ).

### 3.2. Results of the experimental set up representing a drilling scenario in an industrial environment

The SMPS + C 5403 used in the present protocol provides PNC as  $dN/d\ln D_p$  ( $\text{cm}^{-3}$ ), so it has been converted to  $dN/d\log D_p$  ( $\text{cm}^{-3}$ ) by multiplying the values by  $\ln(10)$  therefore allowing comparisons.

An average value of PSD measurement at peak value of C is presented in Fig. 3. PNC shows an increase starting from 62.41 nm with no measured particles for diameters beyond 349.2 nm, approximately, for all samples.

For the comparison of PNC, values corresponding to the initial scan were considered background and subtracted from successive measurements. PP-Talc, PP-WO and PP-MMT showed an increased PNC of 27.27%, 12.20% and 18.88%, respectively, when compared with the particle concentrations of emissions of PP during drilling but such differences were not statistically significant. The emissions of PP-Talc, PP-MMT and PP-WO during post-drilling periods revealed no significant differences when compared with the emissions of PP sample either (Table 2).

In a second step, PNC data were normalized per quantity of drilled mass. The normalized emissions of PP-Talc and PP-MMT exhibited a 35.73% and 31.03% decrease whereas the emissions of PP-WO sample increased 5.34% in comparison with the emissions of the PP sample during drilling, differences not being statistically significant. No significant differences in PNC were observed either during post drilling periods (Table 2).

When PP-Talc was taken as reference sample, a 11.84% and 6.59% decrease and a 63.91% and 7.32% increase was observed during drilling for PP-WO and PP-MMT for the not normalized and normalized data, respectively, none of the differences observed being significant. Changes in the PNC values measured during stabilization periods were not significant either.

### 3.3. Results of the experimental set up representing a drilling scenario in a household environment

The CPC used within the present operational protocol for PNC measurement covers particle size range 1–1000 nm whereas the SMPS covers particle size range 4.61–156.8 nm. This implies that PSD retrieved by the SMPS is just a partial view of the PNC measured by the CPC.

The PSD data obtained by SMPS (Fig. 4) displayed a substantial percentage of the particles released from the PP, PP-WO and PP-MMT samples to be between 5 and 20 nm, whereas the PP-Talc sample emitted larger particle diameters.

PNC data was calculated from CPC as average of emission values recorded during 8 holes drilling (3 min duration; 180 values, one per second) (Table 3). Average values of the fourth minute during which drilling was not performed (stabilization) have also been included in Table 3.

Comparison of the particle concentration measured for emissions corresponding to minutes 1–3 (8 holes drilling) of nanofilled samples exhibited a 29.76% decrease (PP-MMT) or a 50.27% increase (PP-WO) in comparison to the neat PP sample. In the case of PP-Talc a considerable decrease of 60.24% was observed. Differences were significant in all cases ( $p < 0.05$ ). Significant differences ( $p < 0.05$ ) were also observed during the stabilization period (minute 4).

**Table 1**

PNC (C, particles/cm<sup>3</sup>) measured using the industrial milling simulation protocol for 1250 rpm for PP, PP-Talc, PP-WO and PP-MMT samples (CPC Data). Particle levels were determined as an average across all measurements during milling actions of variable durations. The stabilization periods include all particle levels from periods where no milling was conducted and corresponding averages have been calculated. Statistically significant differences have been marked <sup>a</sup> or <sup>b</sup>, with the former referring to the reference sample PP and the latter to PP-Talc.

Activity	PP		PP-Talc		PP-WO		PP-MMT	
	Average (n)	SD	Average (n)	SD	Average (n)	SD	Average (n)	SD
<b>C during milling periods</b>	38.98 (23)	24.02	20.27 <sup>a</sup> (79)	20.46	21.58 <sup>a</sup> (52)	25.48	10.43 <sup>a</sup> (66)	1.56
<b>C during stabilization periods</b>	9.65 (76)	7.34	6.23 <sup>a</sup> (121)	3.01	2.21 <sup>a, b</sup> (148)	1.43	9.42 <sup>a, b</sup> (133)	1.95

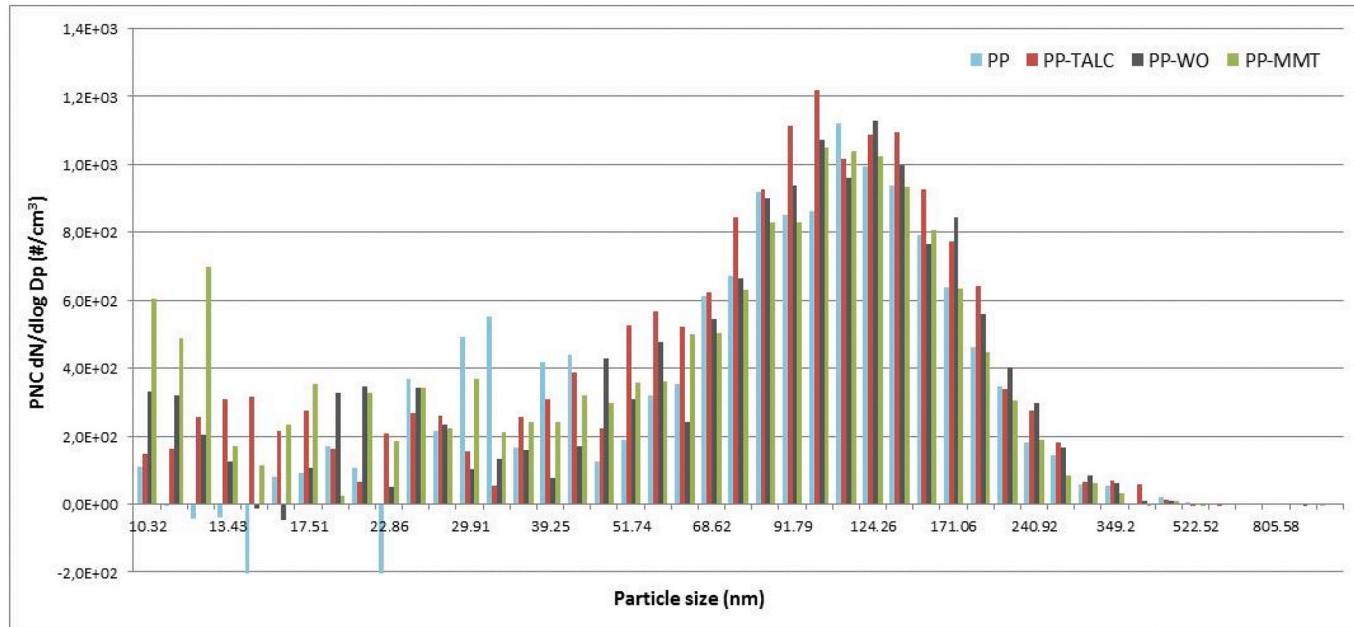


**Fig. 3.** Average of PSD at peak concentration expressed as  $dN/d\log D_p$  (#/cm<sup>3</sup>) having subtracted background concentration corresponding to airborne particle release measurements using the protocol to simulate an industrial drilling process (SMPS + C Data) for PP; PP-Talc; PP-WO and PP-MMT samples.



**Table 2**

PNC (C, particles/cm<sup>3</sup>) measured in the industrial drilling simulating protocol (SMPS + C Data) for the four samples tested: PP; PP-Talc; PP-WO; PP-MMT. Each scan had a fixed duration of 7 min. A total of 4 scans were conducted comprising: an initial scan measuring pre-drilling (background) concentration, a second scan during drilling and two successive scans for particle stabilization. PP samples.

Activity	Scan	Time (min)	Raw Data		Removing Background Values Data		Normalized per Mass Data	
			Average (n = 3)	SD	Average (n = 3)	SD	Average (n = 3)	SD
C pre-drilling (background)	1	0–7	1259.94	123.60				
C during drilling	2	7–14	1834.77	152.87	574.85	264.05	2454.16	1089.37
C during stabilization	3	14–21	2022.87	101.64	762.93	168.45	3266.94	691.09
	4	21–28	1747.65	204.74	293.96	219.40	2096.27	537.32
mass drilled (g)			0.23	0.00				
Activity	Scan	Time (min)	Raw Data		Removing Background Values Data		Normalized per Mass Data	
			Average (n = 4)	SD	Average (n = 4)	SD	Average (n = 4)	SD
C pre-drilling (background)	1	0–7	830.04	271.97				
C during drilling	2	7–14	1561.63	260.96	731.60	80.19	1577.17	148.01
C during stabilization	3	14–21	1828.45	281.15	998.42	92.57	2154.38	185.95
	4	21–28	1749.16	315.91	919.13	123.65	1984.34	264.65
mass drilled (g)			0.46	0.02				
Activity	Scan	Time (min)	Raw Data		Removing Background Values Data		Normalized per Mass Data	
			Average (n = 4)	SD	Average (n = 4)	SD	Average (n = 4)	SD
C pre-drilling (background)	1	0–7	901.06	63.57				
C during drilling	2	7–14	1546.02	148.41	644.97	133.76	2585.22	1445.41
C during stabilization	3	14–21	1715.05	156.07	814.00	116.37	3576.66	2644.51
	4	21–28	1637.55	255.93	736.49	251.12	3080.03	1953.81
mass drilled (g)			0.32	0.18				
Activity	Scan	Time (min)	Raw Data		Removing Background Values Data		Normalized per Mass Data	
			Average (n = 4)	SD	Average (n = 4)	SD	Average (n = 4)	SD
C pre-drilling (background)	1	0–7	818.13	254.73				
C during drilling	2	7–14	1501.51	209.33	683.38	184.06	1692.63	324.34
C during stabilization	3	14–21	1642.96	124.37	824.83	173.05	2134.43	790.28
	4	21–28	1504.01	55.49	685.88	251.71	1795.49	793.16
mass drilled (g)			0.43	0.17				

In view of the results obtained, the addition of nanofillers to the PP matrix can have an increasing or a decreasing effect (PP-WO and PP-MMT, respectively) in C measured for sample's emissions when compared to the emissions of the neat PP sample under the conditions tested. The addition of talc to the PP matrix implies a decrease in C measured during mechanical degradation under the conditions tested.

When the comparison was carried out taking PP-Talc as reference sample significant differences ( $p < 0.05$ ) were observed in the C of released particles, increasing 277.93% and 76.67% for PP-WO and PP-MMT, respectively. During the stabilization period a significant decrease of 28.83% ( $p < 0.05$ ) was observed for the PP-WO sample only.

#### 4. Discussion

Three operational protocols have been developed to simulate different real-world scenarios for composites and nanocomposites including: industrial milling and drilling and household drilling. Changes in particles emission behavior of mechanically degraded PP samples made of PP only or compounded with different types of fillers, including talc and two types of nanoclays, have been investigated under confined conditions.

No significant differences have been observed in the particle release measurements carried out within the industrial drilling scenario for any of the possible comparisons, both in the case of normalized and not normalized data. The results obtained indicate that all samples released particles in the nanosize range. Bello et al. (2010) investigated the generation of nanoscale and submicron particles during solid core drilling of fibre composites containing carbon nanotubes (CNT) and their CNT-free counterparts and concluded that drilling can generate significant exposures to nanoscale and submicron particles for all composites independently of the presence of CNT, in agreement with the results provided by the industrial drilling scenario. Similarly, Wohlleben et al. (2011) reported no significant changes in the concentrations measured during sanding of reference materials without nanofillers and CNT containing nanocomposites.

Both in the industrial milling and household drilling scenarios significant differences were observed when PP sample was taken as a reference, but the tendencies observed were not consistent, being PNC lower for all the comparisons carried out except in the case of the 50.27% increase of PP-WO emissions measured during the household drilling scenario. When PP-Talc was taken as reference, significant differences were observed for the emissions of the two nano-reinforced samples measured during the stabilization period of the industrial milling scenario whereas in the case of the household drilling scenario, significant differences were observed in the

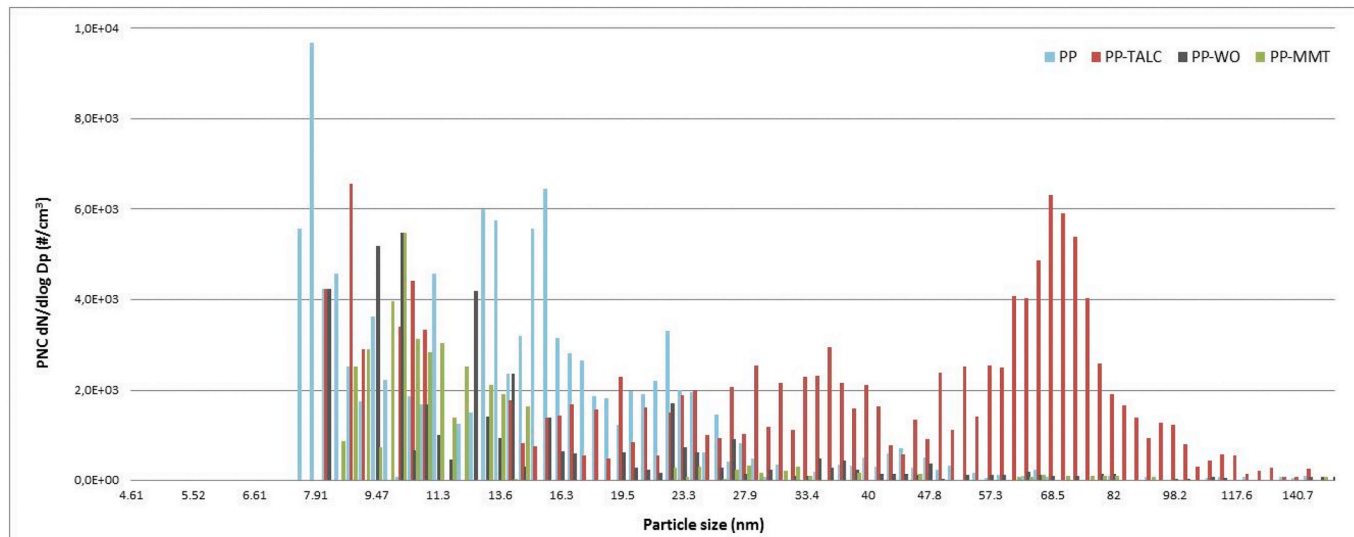


**Fig. 4.** Average of PSD at peak concentration expressed as  $dN/d\log D_p$  ( $\#/cm^3$ ) of particles emitted during the implementation of a protocol simulating a household drilling process (SMPS Data) for the four samples tested: PP; PP-Talc; PP-WO and PP-MMT.

**Table 3**

PNC (C, particles/cm<sup>3</sup>) measured in the household drilling protocol (CPC data) for the four samples tested: PP; PP-Talc; PP-WO and PP-MMT. Particle concentration was measured during 8 holes drilling in a period comprising 3 min (C during drilling). Subsequently, measurements were conducted during one minute, allowing particles to stabilize (C during stabilization). Statistically significant differences have been indicated as <sup>a</sup> when reference sample was PP or <sup>b</sup> in the case of PP-Talc.

Activity	Scan N// Time (min)	PP		PP-Talc		PP-WO		PP-MMT	
		Average (n)	SD	Average (n)	SD	Average (n)	SD	Average (n)	SD
<b>C during drilling</b>	1–3	501.44 (180)	178.94	199.37 <sup>a</sup> (180)	28.68	753.49 <sup>a,b</sup> (180)	154.82	352.23 <sup>a, b</sup> (180)	80.68
<b>C during stabilization</b>	4	292.46 (60)	24.17	136.32 <sup>a</sup> (60)	23.49	97.01 <sup>a,b</sup> (60)	61.82	139.89 <sup>a</sup> (60)	28.91

concentrations measured during drilling for both PP-WO and PP-MMT and for the PP-WO sample only during the stabilization period. [Sachse et al. \(2012\)](#) evaluated the influence of nanoclay on mechanical drilling of polyamide 6 composites in terms of particles generation and concluded that the presence of nanoclay in the composition of the sample led to a significantly lower total particle concentration during drilling, which we have observed as well in the case of the industrial milling (when the PP sample was taken as a reference) and in the household drilling scenarios.

Previous studies concerned with particle release assessment during mechanical degradation of nanocomposites have so far not produced consistent tendencies across different types of degradation. In the present study we have as well not observed a consistent pattern in the particle emissions profile of composite samples that would concisely confirm a significant filler effect. This was true if pure PP was taken as a comparative reference, as well as for PP-Talc.

It is possible that factors other than the presence or absence of micro- or nano-fillers are at the origin of the differences observed, such as the specific scenario, properties of different test equipment or differences in characteristics of instrumentation employed for the measurement of airborne particle release. The operational parameters used for each of the developed scenarios have been summarized in [Table 4](#).

Standardized equipment for the physical degradation of nanocomposite samples exists e.g. in the case of the Taber Abraser, on the basis of which different wear tests have been developed (e.g., DIN 53754:1977, DIN 68861–2:1981, ISO 5470–1:1999, and ASTM D 4060–95:2007). In fact, this type of device has been used widely in previous life cycle oriented research studies ([Schlagenhauf et al., 2012](#); [Wohlleben et al., 2011](#); [Vorbau et al., 2009](#), to cite a few). In contrast to the drilling/milling approaches discussed here, the Taber Abraser exerts a continuous degradation action on the sample (i.e. particles are emitted in a continuous fashion), whereas milling or drilling generate shorter term peaks of emitted particles that are temporally aligned with respective mechanical degradation events. According to [Schutz and Morris \(2013\)](#), the level of particle release from machining depends on the amount of energy that is invested in the process. In the household drilling scenario, the drill was manually operated hindering the calculation and comparability of the energy input. Furthermore, thermal and mechanical degradation of composite samples are two closely related processes, which means that variations in the measurements of released particles cannot solely be attributed to the mechanical process. Variations in the selected spindle speed and/or feed rate can cause differences in the heat generated by the process, which can cause the material to melt and, consequently, emit particulate vapors that tend to re-condensate and adhere to other material surfaces, hence decreasing the

**Table 4**

Comparison of the three simulated scenarios.

	Industrial Milling	Industrial Drilling	Household Drilling
<b>Machining instrument</b>	Aciera F3 Universal Mill (Anglo-Swiss Tools, UK)	CNC machine (ad hoc designed prototype) Drill bit diameter 3.5 mm	Drill model 4000 from Dremel (Wisconsin, USA) Drill bit diameter 3.5 mm
<b>Spindle speed</b>	1250 rpm	8500 rpm	10000 rpm
<b>Feed rate</b>	16 mm/min	200 mm/min	78 mm/min
<b>Cutting speed</b>	0.654 m/s	1.558 m/s	1.833 m/s
<b>Instrumentation used for airborne particle measurement</b>	OPS Model 3330 from TSI, Inc. 16 Channels [300–10000 nm particle size] CPC Model 3007 from TSI, Inc. 1 Channel [10–1000 nm particle size]	SMPS + C Model 5403 from Grimm Aerosol (Ainring, Germany). Instrument includes a classifier type Vienna long U-DMA. 44 Channels [11.1–1083.8 nm particle size]	CPC Model 3783 from TSI, Inc. [1–1000 nm particle size] SMPS Model 3080 from TSI, Inc. Instrument includes an electrostatic classifier with Differential Mobility Analyser (DMA) [4.61–156.8 nm particle size]
<b>Background particles</b>	The entrance and exit of the Experiment Section have been equipped with HEPA filters, which each retain >99.97% of all particles	HEPA filters (category H14) were used. Measures undertaken in scans 1 and 2, ie, prior the drilling process had started have been considered background samples. Such particles have been eliminated in the normalization process.	TSI 99.97% retention HEPA Capsule Filters used to attain a negligible background
<b>Additional information</b>	<a href="#">Schutz and Halliburton (2010)</a>	<a href="#">Gendre et al. (2016)</a>	<a href="#">Starost et al., 2017a, 2017b</a>

number of emitted particles overall. In fact, [Ding et al \(2017a,b\)](#) having assessed the airborne emissions of drilling and sawing polyurethane nanocomposites referred that the sawing tests generated relatively low particle number concentrations in comparison with the drilling tests. However, the sawing process produced intense heat and, consequently, polymer fumes.

Concerning the instrumentation used for particle release measurements, there were also vast differences in the PSD detection ranges. The SMPS used in the protocol simulating household drilling measured particles up to 156.8 nm, which is in contrast with the instrumentation used by the protocols simulating industrial environments which covered particle sizes up to 1000 nm. This leaves the question if these limited size ranges do only reveal a partial picture of the overall particle release. In fact, the protocol simulating an industrial milling did only detect above-particle-background object concentrations for particles <300 nm in all samples investigated, which was also confirmed by the results obtained in the industrial drilling scenario. The limited PSD of the SMPS used in the household drilling protocol is therefore noted as a potential impediment for the comparison of results obtained.

The difficulty of our study relays on the fact that no guidelines or internationally accepted protocols exist to streamline the exposure assessment of ENMs from solid polymer nanocomposites in the framework of a life cycle perspective. Standards should not only pursue how to mechanically degrade the sample, but they should also focus on the exposure assessment that is associated with detecting and characterizing emitted particles. The OECD emission scenario documents on plastic additives ([OECD, 2014](#); [OECD, 2019](#)) represent suitable starting points with this purpose, ENMs being classified as “fillers”.

All the three different protocols we have developed for scenario simulation have taught us several lessons. From the milling scenario we have learned that for machining procedures that are not carried out on a continuous approach (several holes drilling, for instance) the exact timing during which the sample is mechanically degraded should be recorded in order to be able to correlate the airborne particle emissions with the sample treatment process. For the same scenario, we have proposed a mathematically sound approach to integrate measurements from two different instruments. From the industrial drilling protocol we have learned that an improved approach to comparing the data obtained from different scenarios would be to normalize the mass of emissions measured in the nanometer range with respect to the total quantity of material removed during the mechanical degradation process. With such purpose, samples should ideally be weighted before and after the mechanical degradation experiment. Finally, from the household drilling process we have learned that a pre-requisite to judge the soundness of the obtained data is that the measurement ranges of the instrumentation used for released particle assessment in different scenarios are similar, so as to be able to retrieve comparable data. An additional lesson we have learned from the household drilling protocol is that automatically operated instruments should be prioritized in contrast to manual instruments with the aim of minimizing possible variations of the energy input applied in the machining process.

The outcomes of the scenarios that we have simulated are transferable to similar processes in realistic environments including the workplace (industrial milling, drilling) or a consumer use (household drilling). In particular, the drilling process is largely used in composite and nanocomposite materials processing playing a major role in various industries from automotive to aerospace. In this context, [Faraz et al. \(2009\)](#) referred that 55000 holes are generally required to be drilled in a complete single unit production of the Airbus A350 aircraft. The time frames that we have considered in this study range from 3 to 7 min in the case of the household and industrial drilling, respectively, and approximately 50 min in the case of milling. The exposure to released airborne particles derived from the machining of nanocomposites considerably increases during an average 8 h workday.

The stability of airborne nanoparticle agglomerates is another important parameter in simulated scenarios for nanomaterial release and associated human exposure. The mechanisms of particle agglomeration include physical interlock (rough surface, entangled surface shapes, or chain-like, branched structure), electric forces (van der Waals, conductive/non-conductive), magnetic forces (ferromagnetic, induced magnetic) and soft bridging (sticky surface, liquid film, organic functional groups) ([Schneider and Jensen, 2009](#)). It is probable that agglomerated airborne particles break up into smaller agglomerates, or even primary particles, when subjected to larger dispersion forces during release, transport along exposure routes, and during inhalation ([Li and Edwards, 1997](#); [Li et al., 1996](#)). The three scenarios that we have simulated have been carried out in confined conditions limiting deagglomeration processes which could have potentially led to an increased PNC.

Future studies should ideally complement particle release measurements with particle characterization (e.g. microscopical/chemical analysis) in order to determine if and in what form the nanofillers are released. Furthermore, the (eco)toxicological potential of released nanoobjects should be investigated as it might not correspond to that of the pristine ENM or to that of the matrix in which it is integrated. In fact, [Wagner et al. \(2018\)](#) concluded that byproducts generated by the thermal degradation of a polymer polylactic acid-based nanocomposite containing a functionalized MMT could pose a health risk to human lung epithelial cells.

In conclusion, in the present study we have developed three independent protocols with the aim of assessing whether nanoadditivated compositions convey a higher associated exposure towards released nanoobjects in contrast to the traditionally micro-reinforced or neat samples used as a reference during machining operations. Our results have shown that mechanical degradation of PP, PP-Talc, PP-WO and PP-MMT samples leads to the release of nanosized particles. Results suggest that it is not possible to describe the effects of adding nano-sized fillers to PP by a single trend that can be applied across a whole range of different scenarios. There is consequently an urgent need to standardize the exposure assessment of ENMs released from nanocomposites when exposed to different wear and tear or machining scenarios, as they emerge at different stages of their life cycle.

## Declaration of competing interest

The authors declare that they have no known competing financial interests or personal relationships that could have appeared to influence the work reported in this paper.

## Acknowledgements

This work was supported by the LIFE Programme of the European Commission under Grant LIFE11 ENV/ES/596 for the SIRENA project. The contribution of the CSIRO was financially supported by the Nanosafety Stream of the Advanced Materials Transformational Capability Platform (AMTCP). Work at UPV/EHU was funded by a grant to consolidated research groups of the Basque Government (IT1302-19).

## Appendix A. Supplementary data

Supplementary data to this article can be found online at <https://doi.org/10.1016/j.jaerosci.2020.105629>.

## References

- Balkan, O., Ezdes, A., & ir Demire, H. (2010). Microstructural characteristics of glass bead- and wollastonite-filled isotactic-polypropylene composites modified with thermoplastic elastomers. *Polymer Composites*, *31*, 1265–1284. <https://doi.org/10.1002/pc.20953>.
- Bello, D., Wardle, B. L., Zhang, J., Yamamoto, N., Santeufemio, C., Hallock, M., & Virji, M. A. (2010). Characterization of exposures to nanoscale particles and fibers during solid core drilling of hybrid carbon nanotube Advanced composites. *International Journal of Occupational and Environmental Health*, *16*, 434–450. <https://doi.org/10.1179/107735210799159996>.
- Ding, Y., Kuhlbusch, T. A., Van Tongeren, M., Sánchez Jiménez, A., Tuinman, I., Chen, R., Larraza Alvarez, I., Mikolajczyk, U., Nickel, C., Meyer, J., Kaminski, H., Wohlleben, W., Stahlmecke, B., Clavaguera, S., & Riediker, M. (2017a). Airborne engineered nanomaterials in the workplace—a review of release and worker exposure during nanomaterial production and handling processes. *Journal of Hazardous Materials*, *322*(Pt A), 17–28. <https://doi.org/10.1016/j.jhazmat.2016.04.075>.
- Ding, Y., Wohlleben, W., Boland, M., Vilsmeier, K., & Riediker, M. (2017b). Nano-object release during machining of polymer-based nanocomposites depends on process factors and the type of nanofiller. *Annals of Work Exposures and Health*, *61*, 1132–1144. <https://doi.org/10.1093/annweh/wxx081>.
- Ding, Q., Zhang, Z., Wang, C., Jiang, J., Li, G., & Mai, K. (2012). Crystallization behavior and melting characteristics of wollastonite filled bisotactic polypropylene composites. *Thermochimica Acta*, *536*, 47–54. <https://doi.org/10.1016/j.tca.2012.02.023>.
- Duncan, T. (2015). Release of engineered nanomaterials from polymer nanocomposites: The effect of matrix degradation. *ACS Applied Materials & Interfaces*, *7*, 20–39. <https://doi.org/10.1021/am5062757>.
- Faraz, Al, Biermann, D., & Weinert, K. (2009). Cutting edge rounding: An innovative tool wear criterion in drilling CFRP composite laminates. *International Journal of Machine Tools and Manufacture*, *49*, 1185–1196. <https://doi.org/10.1016/j.ijmactools.2009.08.002>.
- Froggett, S. J., Clancy, S. F., Boverhof, D. R., & Canady, R. A. (2014). A review and perspective of existing research on the release of nanomaterials from solid nanocomposites. *Particle and Fibre Toxicology*, *11*, 1–28. <https://doi.org/10.1186/1743-8977-11-17>.
- Gendre, L., Marchante, V., Abhyankar, H. A., Blackburn, K., Temple, C., & Brighton, J. L. (2016). Development of CNC prototype for the characterization of the nanoparticle release during physical manipulation of nanocomposites. *J. Environ. Sci. Health, A*, *51*, 495–501. <https://doi.org/10.1080/10934529.2015.1128720>.
- Gonzalez, L., Lafleur, P., Lozano, T., Morales, A. B., García, R., Angeles, M., Rodriguez, F., & Sanchez, S. (2014). Mechanical and thermal properties of polypropylene/montmorillonite nanocomposites using stearic acid as both an interface and a clay surface modifier. *Polymer Composites*, *35*, 1–9. <https://doi.org/10.1002/pc.22627>.
- International Organization for Standardization, ISO/TC 61/SC 2 Mechanical behaviour. (2019). *ISO 527-1:2019 – plastics. Determination of tensile properties. Part 1: General principles*.
- Janer, G., Fernández-Rosas, E., Mas Del Molino, E., González Gálvez, D., Vilar, G., López-Iglesias, C., Ermini, V., & Vázquez-Campos, S. (2013). *In vitro* toxicity of functionalized nanoclays is mainly driven by the presence of organic modifiers. *Nanotoxicology*, *8*, 279–294. <https://doi.org/10.3109/17435390.2013.776123>.
- Jansz, J. (1999). Polypropylene in automotive applications. In J. Karger-Kocsis (Ed.), *Polypropylene. Polymer Science and technology series* (Vol. 2, pp. 643–651). Dordrecht: Springer. [https://doi.org/10.1007/978-94-011-4421-6\\_87](https://doi.org/10.1007/978-94-011-4421-6_87).
- Li, W. I., & Edwards, D. A. (1997). Aerosol particle transport and deaggregation phenomena in the mouth and throat. *Advanced Drug Delivery Reviews*, *26*, 41–49. [https://doi.org/10.1016/s0169-409x\(97\)00509-7](https://doi.org/10.1016/s0169-409x(97)00509-7).
- Li, W. I., Perzl, M., Heyder, J., Langer, R., Brain, J. D., Englmeier, K. H., Niven, R. W., & Edwards, D. A. (1996). Aerodynamics and aerosol particle deaggregation phenomena in model oral-pharyngeal cavities. *Journal of Aerosol Science*, *27*, 1269–1286. [https://doi.org/10.1016/S0021-8502\(97\)86865-6](https://doi.org/10.1016/S0021-8502(97)86865-6).
- OCDE. (2014). *Plastic additives, series on emission scenario documents* (n° 3). Paris: Editions OCDE. <https://doi.org/10.1787/9789264221291-en>.
- OECD. (2019). *Complementing document to the emission scenario document on plastic additives: Plastic additives during the use of end products. Series on Emission Scenario Documents* (n° 38). Paris: Editions OCDE.
- Sachse, S., Silva, F., Zhu, H., Irfan, A., Leszczyńska, A., Pielichowski, K., Ermini, V., Blazquez, M., Kuzmenko, O., & Njuguna, J. (2012). The effect of nanoclay on dust generation during drilling of PA6 nanocomposites. *Journal of Nanomaterials*, *1*–8. <https://doi.org/10.1155/2012/189386>.
- Salas-Papayanopolos, H., Morales, A. B., Lozano, T., Barbosa, A., Diaz, N., Lafleur, P. G., Laria, J., Sanchez, S., Rodriguez, F., Martínez, G., & Cerino, F. (2014). Improved toughness of polypropylene/wollastonite composites. *Polymer Composites*, *35*, 1184–1192. <https://doi.org/10.2417/spepro.005309>.
- Schlagenhauf, L., Chu, B. T. T., Buha, J., Nüesch, F., & Wang, J. (2012). Release of carbon nanotubes from an epoxy-based nanocomposite during abrasion process. *Environmental Science and Technology*, *46*, 7366–7372. <https://doi.org/10.1021/es300320y>.
- Schlagenhauf, L., Nüesch, F., & Wang, J. (2014). Release of carbon nanotubes from polymer nanocomposites. *Fibers*, *2*, 108–127. <https://doi.org/10.3390/fib2020108>.
- Schneider, T., & Jensen, K. A. (2009). Relevance of aerosol dynamics and dustiness for personal exposure to manufactured nanoparticles. *Journal of Nanoparticle Research*, *11*, 1637–1650. <https://doi.org/10.1007/s11051-009-9706-y>.
- Schutz, J., & Halliburton, B. (2010). Synthetic aerosols from fine carbon nanotubes of 10 nanometres diameter. In *Proceedings of the 2010 international Conference on nanoscience and nanotechnology (ICONN). 22-26 february 2010, Sydney, Australia* (pp. 7–9). IEEE. <https://doi.org/10.1109/ICONN.2010.6045256>.
- Schutz, J., & Morris, H. (2013). *Investigating the emissions of nanomaterials from composites and other solid articles during machining processes* (Report) CSIRO. Canberra: Safe Work Australia.
- Starost, K., Frijns, E., Van Laer, J., Faisal, N., Egizabal, A., Nelissen, I., Elizetxea, C., Blázquez, M., & Njuguna, J. (2017b). Assessment of nanoparticles release into the environment during drilling of carbon nanotubes/epoxy and carbon nanofibres/epoxy nanocomposites. *Journal of Hazardous Materials*, *340*, 57–66. <https://doi.org/10.1080/02786826.2017.1330535>.
- Starost, K., Frijns, E., Van Laer, J., Faisal, N., Egizabal, A., Nelissen, I., Elizetxea, C., Blázquez, M., & Njuguna, J. (2017a). The effect of nanosilica (SiO<sub>2</sub>) and nanoalumina (Al<sub>2</sub>O<sub>3</sub>) reinforced polyester nanocomposites on aerosol nanoparticle emissions into the environment during automated drilling. *Aerosol Science and Technology*, *51*, 1035–1046. <https://doi.org/10.1080/02786826.2017.1330535>.
- Verma, N. K., Moore, E., Blau, W., Volkov, Y., & Babu, P. R. (2012). Cytotoxicity evaluation of nanoclays in human epithelial cell line A549 using high content screening and real-time impedance analysis. *Journal of Nanoparticle Research*, *14*, 1–11. <https://doi.org/10.1007/s11051-012-1137-5>.

- Vorbau, M., Hillemann, L., & Stintz, M. (2009). Method for the characterization of the abrasion induced nanoparticle release into air from surface coatings. *Journal of Aerosol Science*, 40, 209–217. <https://doi.org/10.1016/j.jaerosci.2008.10.006>.
- Wagner, A., White, A., ChioTang, M., Agarwal, S., Stueckle, T. A., Sierros, K. A., Rojanasakul, Y., Gupta, R. K., & Dinua, C. Z. (2018). Incineration of nanoclay composites leads to byproducts with reduced cellular reactivity, 10709 *Nature Scientific Reports*, 8, 1–15. <https://doi.org/10.1038/s41598-018-28884-y>.
- Wohlleben, W., Brill, S., Meier, M. W., Mertler, M., Cox, G., Hirth, S., von Vacano, B., Strauss, V., Treumann, S., Wienche, K., Ma-Hock, L., & Landsiedel, R. (2011). On the lifecycle of nanocomposites: Comparing released fragments and their in-vivo hazards from three release mechanisms and four nanocomposites. *Small*, 7, 2384–2395. <https://doi.org/10.1002/sml.201002054>.